NEAR-THRESHOLD FATIGUE CRACK GROWTH BEHAVIORS IN AIR AT ROOM TEMPERATURE FOR VARIOUS STAINLESS STEELS

S. Matsuoka, S. Nishijima, C. Masuda and S. Ohtsubo

National Research Institute for Metals 2-3-12, Nakameguro, Meguroku, Tokyo 153, Japan

ABSTRACT

Near-threshold fatigue crack growth behaviour is investigated for four stainless steels of ferritic 17Cr, martensitic 12Cr, and austenitic 18Cr-8Ni and 25Cr-20Ni in laboratory and dry air at room temperature. The stainless steels are free from oxide-induced closure because large amount of chromium in the stainless steels assures formation of the passive film on the fracture surface and thus, prevents oxide thickening within the crack. In laboratory air, therefore, ΔK_{th}-values for stainless steels are lower when compared with those for carbon or low alloy steels with similar strength levels. Dry air does not influence the near-threshold crack growth behaviors for stainless steels, while it eliminates the excess oxide debris from fracture surface of carbon or low alloy steels and reduces their ΔK_{th}-values to the level of stainless steels. In austenitic stainless steels, furthermore, ΔK_{th}- values are significantly reduced and fracture surfaces near ΔK_{th} are markedly crystallographic at lower load ratios, compared to ferritic and martensitic stainless steels. Such phenomena are related to strain-induced martensitic transformation peculiar to the austenitic stainless steel.

KEYWORDS

Near-threshold fatigue crack growth; oxide-induced closure; stainless steels; chromium; passive film; strain-induced martensitic transformation.

INTRODUCTION

Near-threshold fatigue crack growth behavior has been found to be influenced by oxide-induced closure in addition to plasticity-induced closure (Stewart,1980; Suresh and others,1980). At lower load ratios, the threshold stress intensity, ΔK_{th}, is considerably higher in laboratory air than in dry inert gas atmospheres such

as hydrogen and helium. In laboratory air, which contains water vapor, oxide debris is generated and thickened within the crack by fretting oxide mechanisms resulting from plasticity-induced closure. This oxide debris raises crack closure level and thus reduces the effective ΔK. At higher load ratios where there is no plasticity-induced closure, ΔK_{th} is independent of atmospheres.

In this study, the near-threshold fatigue crack growth behavior is examined for different stainless steels of type ferritic 17Cr, martensitic 12Cr, and austenitic 18Cr-8Ni and 25Cr-20Ni in laboratory and dry air at room temperature. The determination of ΔK_{th} for these stainless steels is of practical importance because they are often used for critical components of machines and structures. The stainless steels which contain large amount of chromium are expected to be free from oxide-induced closure since the fracture surface would be covered by a thin passive film and thus excess oxide debris would be prevented. In addition, the austenitic stainless steels exhibit the inherent strain-induced martensitic transformation. This microstructual change should affect the near-threshold crack growth behavior.

EXPERIMENTAL PROCEDURES

The materials used were four stainless steels; ferritic SUS430 (17Cr), martensitic SUS403 (12Cr), and austenitic SUS304 (18Cr-8Ni) and SUH310 (25Cr-20Ni). Their chemical compositions, mechanical properties and heat treatment conditions are listed

Table 1

	C	S_i	M_n	P	S	C_u	N_i	C_r	M_o
SUS430	0.07	0.46	0.60	0.026	0.005	-	0.28	16.75	0.03
SUS304	0.06	0.53	1.11	0.033	0.010	-	9.04	18.23	-
SUH310	0.13	1.09	1.85	0.025	0.009	0.11	20.01	24.80	0.26
SUS403	0.14	0.31	0.66	0.025	0.008	0.03	0.16	11.79	0.15
S25C	0.26	0.23	0.51	0.018	0.024	0.01	0.01	0.02	-
SM50B	0.15	0.37	1.36	0.020	0.005	0.01	0.03	0.02	0.001
A553	0.06	0.17	0.54	0.005	0.006	-	9.10	-	-
S45C	0.43	0.22	0.83	0.017	0.016	0.01	0.01	0.12	-
HT80	0.12	0.26	0.96	0.010	0.004	0.19	1.05	0.45	0.31
SNCM439	0.40	0.25	0.63	0.029	0.020	0.13	1.68	0.68	0.18

Table 2

	σ_y (MPa)	σ_B (MPa)	δ (%)	Micro-* structure	Heat treatment **	Symbols Lab.air	Symbols Dry air
SUS430	303	480	40	F	815°C A	○	◓
SUS304	336	613	60	A	1050°C ST	□	◨
SUH310	271	619	45	A	1050°C ST	◇	◈
SUS403 700T	574	708	24	M	975°C Q AND 700°C T	△	—
SUS403 600T	629	743	22	M	975°C Q AND 600°C T	▽	▼
S25C	362	521	37	F/P	845°C A	●	◑
SM50B	372	530	25	F/P	AS HOT ROLLED	▬	▬
A553	698	745	37	M/A	575°C T	■	◧
S45C	623	774	22	M	845°C Q AND 600°C T	▲	◭
HT80	784	843	12	M	570°C T	▼	▽
SNCM439	1060	1080	18	M	845°C Q AND 600°C T	▶	▶

* F Ferrite, A Austenite, M Tempered Martensite, P Pearlite

** A Annealed, ST Solution treated, Q Quenched, T Tempered

in Tables 1 and 2. 403 steel was quenched and tempered at either 600 or 700°C to obtain different strength levels. In the stainless steels, a strong passive film is generally formed on the fracture surface in air when the amount of chromium reaches around 13 percent. In order to compare with fatigue behavior of stainless steels, low alloy steels SM50B, A553, HT80 and SNCM439, and carbon steels S25C and S45C containing small amounts of chromium were also investigated in this study. The strength levels and microstructures of 430 and 403 stainless steels are similar to those of S25C or SM50B and S45C steels, respectively, while such similarities are not realized for 304 and 310 austenitic stainless steels. A553 steel contains 30 percent of austenite and its strength level is much higher than those of austenitic stainless steels.

Fatigue crack propagation experiments were performed with small compact specimens of 25mm width and 5mm thickness at room temperature in laboratory and dry air with relative humidity of 30 to 80% and of 0.0003%, respectively. Testing was carried out on a 50kN vibrophore electromagnetic resonance type machine operating at 160Hz. A special device was employed to compensate the change of specimen compliance during the test and to obtain a small load suitable for the small compact specimen. ΔK_{th}-values were determined at load ratios, $R = P_{min}/P_{max}$, of 0.1, 0.5 and 0.9. ΔK was automatically decreased under combined modes of applied load and backface strain of the compact specimen. In the determination of ΔK_{th} at R = 0.9, the load ratio varied from 0.6 to 0.9 because the minimum load was kept constant and the maximum load decreased. The detailed procedures have been described elsewhere (Nishijima and others,1983).

Fracture surfaces were observed by a scanning electron microscope especially to characterize the oxidation appearance and fractrographic aspect near ΔK_{th}. The thickness of oxide layer on fracture surface was evaluated by Auger spectroscopy.

EXPERIMENTAL RESULTS

Fig. 1 shows da/dN vs ΔK curves and Fig. 2 ΔK_{th} vs R relations for the stainless steels in laboratory and dry air. The data for the carbon and low alloy steels are shown together with some published data (Ohta and others,1977) in the two figures for comparison. The symbols used in Fig. 2 are defined in Table 2. These results could be summarized as in the following.

(1) In comparison of 430 stainless steel with S25C or SM50B steels, ΔK_{th}-values were lower in the stainless steel at lower load ratios of 0.1 and 0.5, but are the same for both types of steels at higher load ratio of 0.9 in laboratory air (Fig. 2a). Reflecting the behavior of ΔK_{th}, at high load ratio the fatigue crack growth curves were identical for the two types of steels, and at low load ratio the growth rates were higher in the stainless steel (Fig. 1a). In dry air, where the excess oxide debris is expected to be prevented, the growth rates for the carbon and low alloy steels were accelerated at low load ratio and their ΔK_{th}-values were equal to those for the stainless steel, while the stainless steel was independent of the environment (Figs. 1b and 2a).

(2) Comparable results are obtained for 304 and 310 stainless steels with A553 steel (Fig. 2b). However, ΔK_{th}-values for 304 and 310 stainless steels were much lower than those for 430 stainless steel at lower load ratios, and thus practically independent of the load ratio. This is due to the fact that the fatigue crack growth curves for 304 and 310 stainless steels at $R \simeq 0.1$ abruptly shifted to the lower ΔK level at $da/dN < 5\times10^{-9}$m/cycle (Fig. 2c). Note that 304 and 310 steels are austenitic and 430 steel ferritic, although these three steels have the same strength levels.

(3) Near-threshold fatigue crack growth behaviors for martensitic 403 stainless steel were dependent on the strength level and

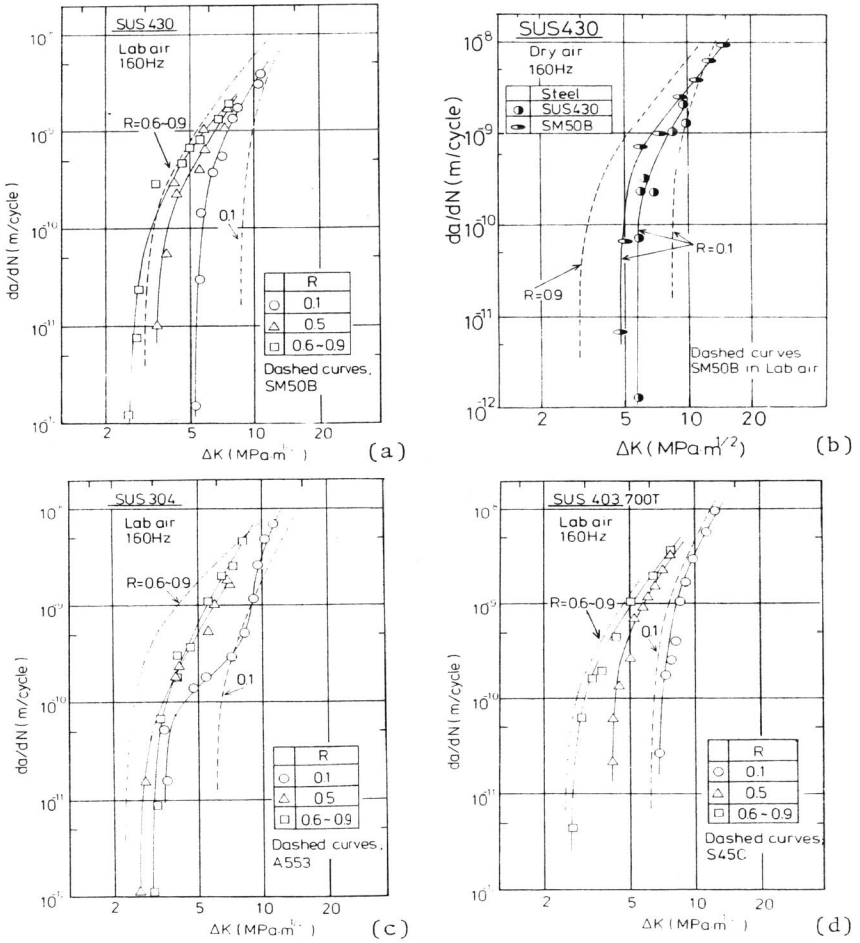

Fig. 1. da/dN vs ΔK curves. (a) and (b) SUS430 in laboratory and dry air. (c) and (d) SUS304 and SUS403 in laboratory air.

environment. In laboratory air, the growth curves and ΔK_{th}-values at R = 0.1 to 0.9 for 403 stainless steel tempered at 700°C were coincident with those for S45C, HT80 and SNCM439 steels (Figs. 1d and 2c). However, ΔK_{th}-values of 403 less steel tempered at 600°C decreased at lower load ratios. Nevertheless, the tensile strength was a little higher than in the same steel tempered at 700°C and much lower than in SNCM439 steel. Dry air test caused a further decrease in ΔK_{th} of 403 stainless steel tempered at 600°C. These are due to the fact that the 403 stainless steel hardly contains a critical chromium content of 13% to form a stable, thin passive film on the fracture surface in air, whereas the other 430, 304 and 310 stainless steels contain more than 18% and are assured of being free from the excess oxide formation (Table 1).

Fig. 3 shows macrographs of fracture surface at $R \simeq 0.1$. In the carbon and low alloy steels such as SM50B, the dark band which may have resulted from the fretting oxidation process was found

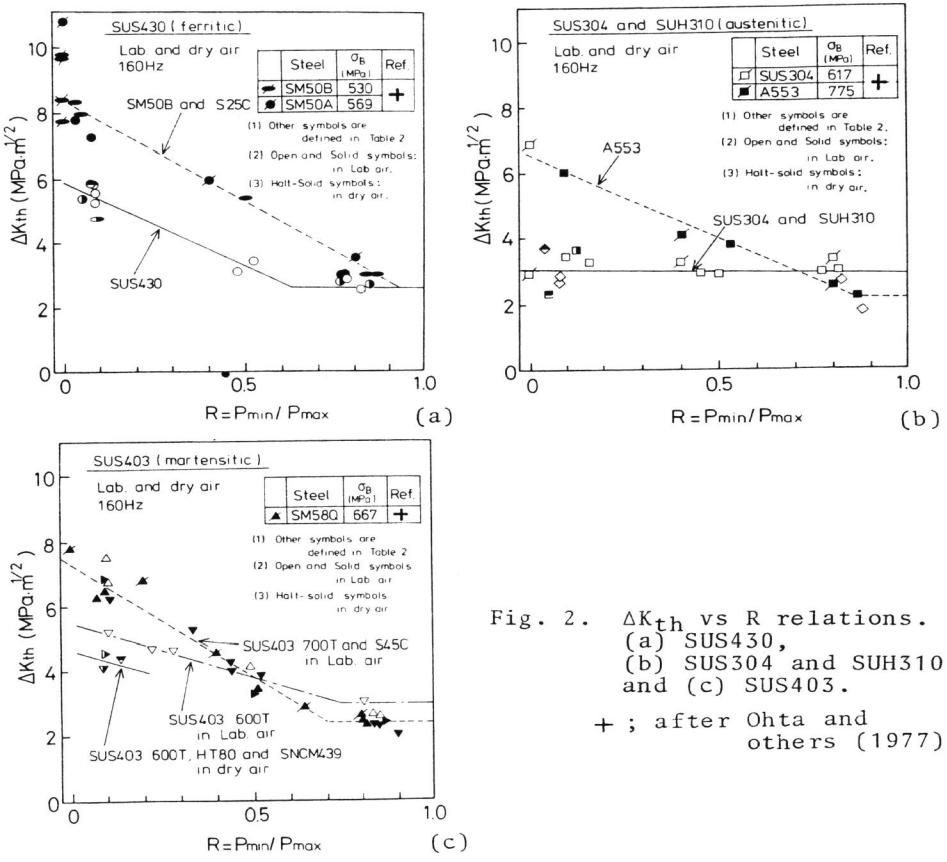

Fig. 2. ΔK_{th} vs R relations. (a) SUS430, (b) SUS304 and SUH310, and (c) SUS403.

+ ; after Ohta and others (1977).

on the near-threshold region in laboratory air, while such a band was not observed in dry air (Figs. 3f & 3g). In 430, 304 and 310 stainless steels, the dark band was not produced even in laboratory air (Figs. 3a & 3b). In 403 stainless steel whose ΔK_{th}-values were dependent on the strength level and environment, a narrow dark band was formed for materials tempered both at 600 and 700°C in laboratory air (Figs. 3c & 3d). The crack front was nearly straight in tempering at 600°C, whereas the crack tunneled ahead in the interior of the specimen in tempering at 700°C. Furthermore, dry air completely eliminated the dark band from the fracture surface of 403 stainless steel tempered at 600°C (Fig. 3e). At $R \simeq 0.9$ where there is no plasticity-induced closure, the dark band did not appear for all the materials.

Scanning electron micrographs near ΔK_{th} at $R \simeq 0.1$ reveal that in SM50B steel the fine-scale transgranular mode was clearly recognized in dry air, while the photograph in laboratory air was not sharp because of excess oxide debris (Figs. 3c & 3d). The oxide debris was not observed in 430 and 304 stainless steels (Figs. 3a & 3b). In addition, the fracture surface for austenitic 304 stainless steel, where the river-like lines appear to change their directions from grain to grain, was more crystallographic than those for ferritic 430 and SM50B steels. At $R \simeq 0.9$, all the materials including the austenitic stainless steels exhibited the fine-scale transgranular mode aspect.

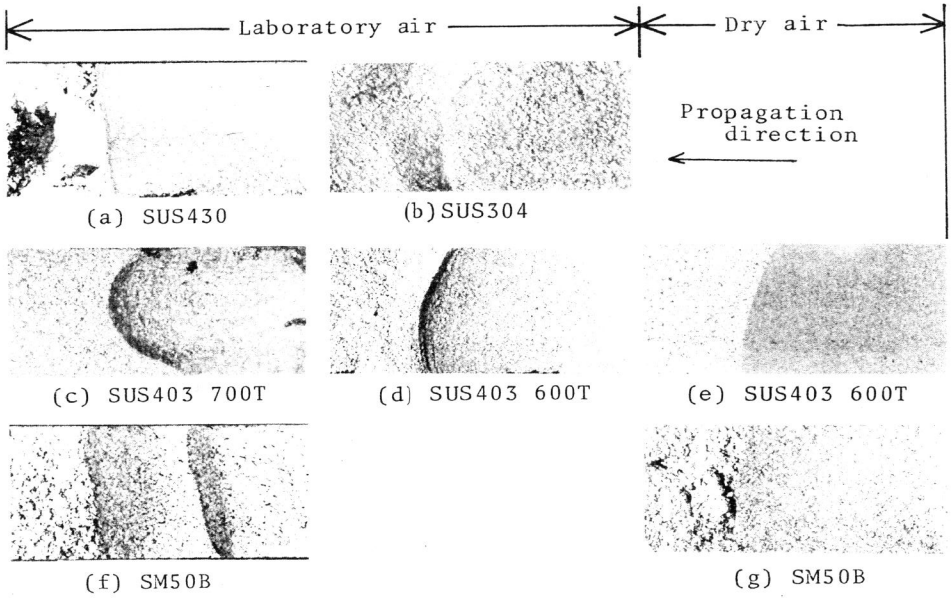

Fig. 3. Macrographs of fracture surfaces at $R \simeq 0.1$
(a) and (b) SUS430 and SUS304 in laboratory air.
(c) and (d) SUS403 tempered at 700 and 600°C in laboratory air and (e) SUS403 tempered at 600°C in dry air.
(f) and (g) SM50B in laboratory and dry air.

The thickness of oxide layer was evaluated by Auger spectroscopy. Fig. 5 shows two examples of Auger electron energy spectra for 430 stainless steel at $R \simeq 0.1$ in laboratory air. The iron peak at 45eV electron energy is influenced by the existence of oxide. That is, the peak is duplex after 2 seconds of argon sputtering where a great amount of oxide still remains (upper curve), while a neat peek is observed when the oxide is mostly eliminated by 120 second sputtering (lower curve). The range of oxygen peak which is in proportion to the amount of oxide decreased with increasing sputter time. In Fig. 6 are shown the variations of oxygen peak range against sputter time for 430 stainless steel and SM50B steel in laboratory air. The oxygen range was normalized by the iron peak range at 704eV. The sputter time was calibrated using a known thickness of iron layer deposited by vacuum evaporation on a nickel plate. The iron layer with 0.18μm thickness was almost removed by 1800 seconds of sputtering. The scale for the depth from fracture surface on the upper horizontal axis of the figure was obtained from this calibration. Fig. 6 suggests that in SM50B steel the oxide thickness near ΔK_{th} is of the oder of 0.1μm at $R \simeq 0.1$ and 0.01μm at $R \simeq 0.09$ in laboratory air. In 430 stainless steel, the oxide film is very thin even at $R \simeq 0.1$ and its thickness is almost the same as that for SM50B steel at $R \simeq 0.9$.

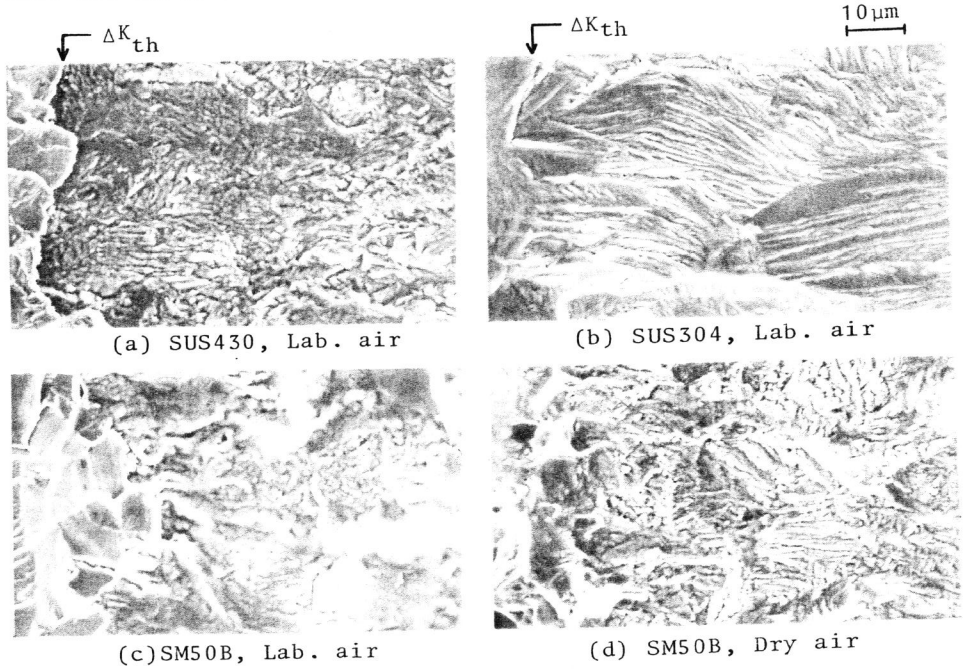

Fig. 4. Scanning electron micrographs at $R \simeq 0.1$.
(a) and (b) SUS430 and SUS304 in laboratory air.
(c) and (d) SM50B in laboratory and dry air.

DISCUSSION

The concept of oxide-induced closure is useful to explain near-threshold fatigue crack growth behaviors in gaseous environments such as air, hydrogen and argon. According to the results for 2.25Cr-1Mo steel with the tensile strength of 610MPa by Suresh and others (1980), ΔK_{th}-values at R = 0.05 were 7.7MPa·√m in moist air and 5.2MPa·√m in dry inert hydrogen. At R = 0.75 where is no plasticity-induced closure ΔK_{th} was almost identical in both atmospheres (≈3.3MPa·√m). The Auger spectroscopic analysis showed that the oxide thickness at ΔK_{th} was of the order of 0.3μm in air at R = 0.05 and less than 0.1μm in hydrogen. At R = 0.75 the thicknesses in both atmospheres were smaller by an order of magnitude. Considering the results in this study with the results by Suresh and others (1980), it is concluded that the stainless steels 430, 304 and 310 containing more than 13%Cr could be free from oxide-induced closure even in moist laboratory air since the thin passive film coats the fracture surface and thus prevents excess oxide debris.

In Fig. 7 are summarized ΔK_{th}-values at R ≈ 0.1 and 0.9 as a function of the tensile strength. ΔK_{th}-values for carbon and low alloy steels in laboratory air decreased with increasing in the strength level at R ≈ 0.1 where both the oxide- and plasticity-induced closures are dominant, while the dependence on the strength level was reduced at R ≈ 0.9 where there is no closure. On the other hand, ΔK_{th}-values for stainless steels and those for carbon and low alloy steels in dry air did not exhibit the strong dependence on the strength level even at R ≈ 0.1 when only the plasticity-induced closure is dominant. These results suggest that the dependence of ΔK_{th} on the strength level would be governed by the oxide-induced closure. In other words, the oxide-induced closure decreases with increases in the strength level, whereas the plasticity-induced closure is less-sensitive

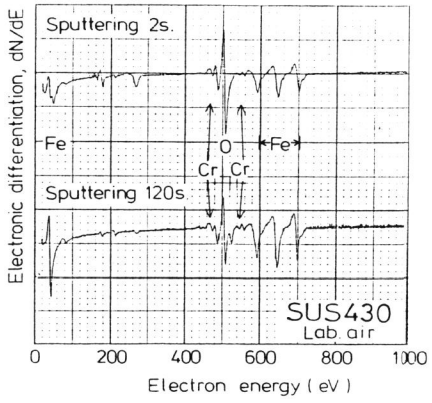

Fig. 5. Auger electron energy spectra for SUS430 steel at R ≈ 0.1.

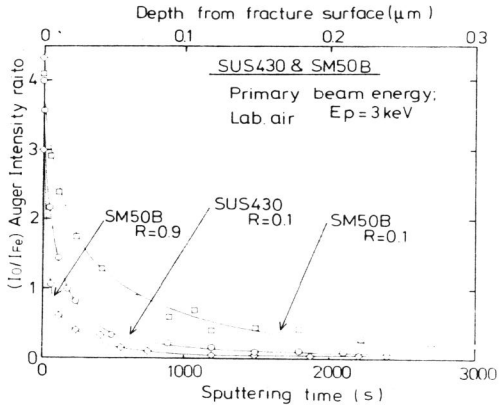

Fig. 6. Evaluation of oxide thickness for SUS430 and SM50B steels.

to the strength level. The latter phenomenon is compatible with the fact that the fatigue crack growth rate is independent of the mechanical properties such as yield and tensile strengths at the mid-range of growth rates, where the plasticity-induced closure is dominant. The former phenomenon about oxide-induced closure might be in connection with the fact that the fretting wear is reduced with the increase in the hardness of materials.

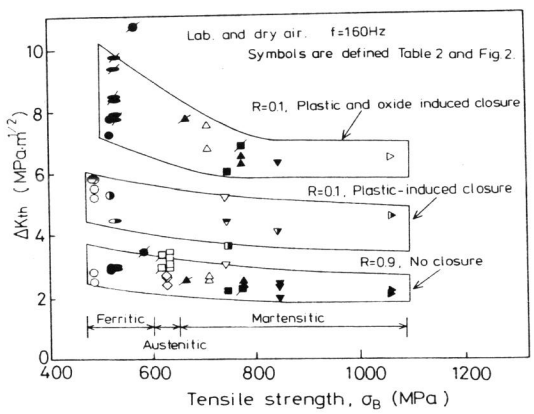

Fig. 7. Dependence of ΔK_{th} on tensile strength.

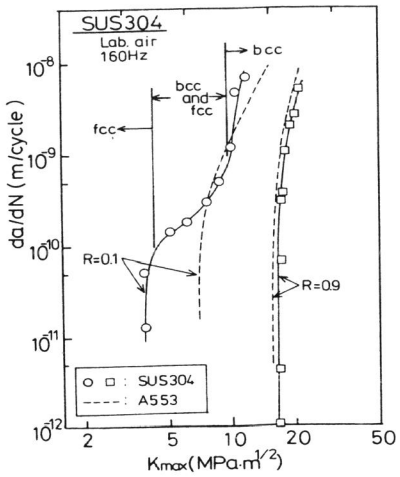

Fig. 8. da/dN vs K_{max} curves for SUS304 steel.

Figs. 1 and 2 furthermore suggest that near-threshold fatigue crack growth behavior for austenitic stainless steels might be affected by a mechanism other than oxide- and plasticity-induced closures. That is, the growth curves at R ≈ 0.1 abruptly shifted to the lower ΔK-level below the critical growth rate and thus ΔK_{th}-values were almost independent on load ratio in austenitic stainless steels. The closure measurement by elastic compliance method, however, revealed that the austenitic stainless steels exhibited an apparent crack closure at R ≈ 0.1, while there was no closure at R ≈ 0.9, being analogous to the other steels. It is natural to correlate such phenomena of austenitic stainless steels with the strain-induced martensitic transformation. This transformation is inherent to the austenitic stainless steel, and results in two effects on the zone ahead of crack tip; the change in the lattice of the material from fcc (austenite) to bcc (martensite) and the formation of excess residual compressive stress due to the cubical expansion.

Fig. 8 shows da/dN vs K_{max} curves for 304 stainless steel and A553 tempered-martensitic steel at R ≈ 0.1 and R ≈ 0.9. It appears that the martensitic transformation might be strongly occured on 304 steel when K_{max} becomes larger than 9.3MPa·√m. The growth rate curves for 304 steel was coincident with those for A553 steel at this range of K_{max}, although the excess residual compressive stress could be produced in the plastic zone

ahead of the crack tip for 304 steel. At $K_{max} < 9.3 MPa \cdot \sqrt{m}$, the growth rate was accelerated on 304 steel as compared with A553 steel. In addition, the fracture surface was more crystallographic in 304 steel than 430 or SM50B steel near ΔK_{th} at $R \simeq 0.1$, where the microstructure ahead of crack tip for 304 steel could be predominantly austenitic (fcc). The crystallographic fracture mode is also formed near ΔK_{th} region on various fcc materials such as aluminium alloy (Kirby and Beevers, 1979), copper (Stanzl and Tschegg,1980) and nickel alloy (Vincent and Remy,1981). ΔK_{th}-values at $R \simeq 0$ are between 2.6 and 3.3 $MPa \cdot \sqrt{m}$ for aluminium alloys (Kirby and Beevers,1979; Pook,1972) and $2.5 MPa \cdot \sqrt{m}$ for copper (Stanzl and Tschegg,1980), which are almost the same as those for the austenitic stainless steels (Fig. 2b). These results imply that near-threshold fatigue crack growth behavior for the austenitic stainless steels would be related to the change of microstructure rather than the formation of excess residual compressive stress ahead of the crack tip. Furthermore, the nickel alloys exhibit a higher ΔK_{th}-values of about $7 MPa \cdot \sqrt{m}$ at $R = 0$ (Pook,1972), nevertheless their Young's modulus is almost equal to that for the steel. In general, the crystallographic fracture mode increases the roughness of fracture surface and results in the increase of crack closure level. The nickel alloy particularly has a tendency to produce large planer intergranular facets (Vincent and Remy,1981). This factor may also be taken into account for the above discussion.

SUMMARY AND CONCLUSION

Near-threshold fatigue crack growth behaviour has been examined for various stainless steels in air at room temperature. In moist laboratory air ΔK_{th}-values for stainless steels were lower than those for carbon or low alloy steels, whereas in dry air ΔK_{th}-values were identical for both types of steels. Such behaviour is a result of the fact that the effect of oxide-induced closure on ΔK_{th} was negligible in stainless steels since the passive film coated the fracture surface and thus prevented the excess oxide debris. Furthermore, the austenitic stainless steels showed a lower ΔK_{th}-level and more crystallograpic fracture mode than the ferritic and martensitic stainless steels at $R \simeq 0.1$. Such phenomena were expected to be connected with the strain-induced martensitic transformation.

REFERENCES

Kirby, B. R. and C. J. Beevers (1979). Fatigue of Engng Mater. and Structures, 1, 203-215.

Nishijima, S., S. Matsuoka and S. Ohtsubo (1983). J. Test. and Eval., 3, 193-201.

Ohta, A., E. Sasaki and M. Kosuge (1977). Trans. of National Research Institute for Metals, Japan, 19, 183-199.

Pook, L. P. (1972). ASTM STP 513, 106-124.

Stanzl, S. and E. Tschegg (1980). Metal Science, 14, 137-143.

Stewart, A. T. (1980). Engng Fract. Mech., 13, 463-478.

Suresh, S., G. F. Zamiski and O. R. Ritchie (1980). Metal Trans., 12A, 1435-1443.

Vincent, J. N. and L. Remy (1981). ICF5, France, 1357-1365.